



## **A novel, automated, quantification of abnormal lung parenchyma in patients with COVID-19 infection: Initial description of feasibility and association with clinical outcome**

Eric Noll, Luc Soler, Mickaël Ohana, Pierre-Olivier Ludes, Julien Pottecher, Elliott Bennett-Guerrero, Francis Veillon, Bernard Goichot, Francis Schneider, Nicolas Meyer, et al.

### **► To cite this version:**

Eric Noll, Luc Soler, Mickaël Ohana, Pierre-Olivier Ludes, Julien Pottecher, et al.. A novel, automated, quantification of abnormal lung parenchyma in patients with COVID-19 infection: Initial description of feasibility and association with clinical outcome. *Anaesthesia Critical Care & Pain Medicine*, 2021, 40 (1), pp.100780. <10.1016/j.accpm.2020.10.014>. <hal-03522161>

**HAL Id: hal-03522161**

**<https://hal.science/hal-03522161v1>**

Submitted on 24 Apr 2023

**HAL** is a multi-disciplinary open access archive for the deposit and dissemination of scientific research documents, whether they are published or not. The documents may come from teaching and research institutions in France or abroad, or from public or private research centers.

L'archive ouverte pluridisciplinaire **HAL**, est destinée au dépôt et à la diffusion de documents scientifiques de niveau recherche, publiés ou non, émanant des établissements d'enseignement et de recherche français ou étrangers, des laboratoires publics ou privés.



Distributed under a Creative Commons CC BY-NC 4.0 - Attribution - Non-commercial use - International License

## **A Novel, Automated, Quantification of Abnormal Lung Parenchyma in Patients with COVID-19 Infection: Initial Description of Feasibility and Association with Clinical Outcome**

Eric NOLL<sup>1,2,3\*</sup>, Luc SOLER<sup>4,5</sup>, Mickael OHANA<sup>6</sup>, Pierre-Olivier LUDES<sup>1,3</sup>, Julien POTTECHER<sup>1,3</sup>, Elliott BENNETT-GUERRERO<sup>7</sup>, Francis VEILLON<sup>8</sup>, Bernard GOICHOT<sup>9</sup>, Francis SCHNEIDER<sup>10</sup>, Nicolas MEYER<sup>11</sup>, Pierre DIEMUNSCH<sup>1,2,3</sup>

1. Department of Anesthesiology and Intensive Care, H  tepi  re Hospital, Strasbourg University Hospital, France
2. Institut Hospitalo-Universitaire "Image-Guided Surgery", Strasbourg University Hospital, Strasbourg, France
3. Equipe d'Accueil 3072, Medical School, Strasbourg University, Strasbourg, France
4. Digestive and endocrine Surgery Department , Nouvel H  pital Civil, Strasbourg, France
5. Visible Patient, Strasbourg, France
6. Department of radiology, Nouvel H  pital Civil, Strasbourg University Hospital, France
7. Department of anesthesiology, Stony Brook Medicine, New-York, USA
8. Department of radiology, H  tepi  re Hospital, Strasbourg University Hospital, France
9. Department of internal medicine, H  tepi  re Hospital, Strasbourg University Hospital, France
10. M  decine Intensive-R  animation, H  tepi  re Hospital, Strasbourg University Hospital, Strasbourg, France.
11. Department of Biostatistics, Strasbourg University Hospital, France

**\*Corresponding Author:** Pr Eric Noll

Department of Anesthesiology and Intensive Care, H  tepi  re Hospital, Strasbourg, France

Email : [eric.noll@chru-strasbourg.fr](mailto:eric.noll@chru-strasbourg.fr)

**A Novel, Automated, Quantification of Abnormal Lung Parenchyma in Patients with COVID-19 Infection: Initial Description of Feasibility and Association with Clinical Outcome**

Funding: institutional support

Keywords: COVID-19, ARDS, CT-scan, triage, severity assessment, infectious disease

## Summary

### Objective:

Ground-glass opacities are the most frequent radiologic features of COVID-19 patients. We aimed to determine the feasibility of automated lung volume measurements, including ground-glass volumes, on the CT of suspected COVID-19 patients. Our goal was to create an automated and quantitative measure of ground-glass opacities from lung CT images that could be used clinically for diagnosis, triage and research.

### Design:

Single centre, retrospective, observational study

### Measurements:

Demographic data, respiratory support treatment (synthesised in the maximal respiratory severity score) and CT-images were collected. Volume of abnormal lung parenchyma was measured with conventional semi-automatic software and with a novel automated algorithm based on voxels X-Ray attenuation. We looked for the relationship between the automated and semi-automated evaluations. The association between the ground-glass opacities volume and the maximal respiratory severity score was assessed.

### Main results:

Thirty-seven patients were included in the main outcome analysis. The mean duration of automated and semi-automated volume measurement process were 15 (2) and 93 (41) min, respectively ( $p = 8.05 \times 10^{-8}$ ). The intraclass correlation coefficient between the semi-automated and automated measurement of ground-glass opacities and restricted normally aerated lung were both superior to 0.99. The association between the automated measured lung volume and the maximal clinical severity score was statistically significant for the restricted normally aerated ( $p = 0.0097$ , effect-size: -385 ml) volumes and for the ratio of ground-glass opacities/restricted normally aerated volumes ( $p = 0.027$ , effect-size: 3.3).

### Conclusion:

The feasibility and preliminary validity of automated impaired lung volume measurements in a high-density COVID-19 cluster was confirmed by our results.

## Introduction

A pandemic involving the severe acute respiratory syndrome coronavirus 2 (SARS-CoV-2) has spread worldwide since December 2019 (1–3). This virus can induce clinical symptoms labelled coronavirus disease 2019 (COVID-19) by the World Health Organization (4). Among the symptoms of COVID-19, acute respiratory failure is one of the most significant, and may lead to severe morbidity and mortality (5–9). COVID-19 is characterised by large person-to-person transmission leading to massive outbreaks of acutely ill patients in infected areas (7, 10, 11). In this context, optimising triage for suspected COVID-19 patients is critical (12). Particularly, assessing the severity of lung injury in each case is challenging (13). Oxygen requirement is a useful tool, but in many patients, may not be directly associated with the magnitude of lung injury, e.g. concomitant heart failure if there is ventricular dysfunction or pulmonary embolism. In addition, there is an unmet need for a quantitative measure of lung injury for use in clinical studies, e.g. as part of eligibility criteria, endpoint of treatment, or as a baseline potential confounder.

Lung abnormality on chest CT has been reported in COVID-19 cases (14, 15). Being widely available, CT is broadly used as a routine diagnostic tool in addition to RT-PCR sampling (16). CT is used in some patients to qualitatively quantify (17, 18) the extent of lung parenchymal lesions.

In this descriptive study, we aimed at assessing the feasibility of a novel automated quantification process for one of the most significant pulmonary abnormalities observed in COVID-19, *i.e.* ground-glass opacities (19). We hypothesised that automated quantification of ground glass opacity is feasible, and that more lesions are associated with worse clinical outcome.

## Methods

### Study design and participants

This is a retrospective study performed at the Hautepierre Hospital, a French University Hospital in Strasbourg France, a high-density case cluster during the COVID-19 outbreak. The study was designed and reported in order to maximise fulfilling the STROBE (Strengthening the Reporting of the OBservational studies in Epidemiology) statement (20). As per French regulatory law (21), this study was considered as observational research on routine clinical data and therefore the need for informed consent was waived as confirmed by the Institutional Review Board Approval (approval # IRB 00010254-2020-053, French Society of Anaesthesia and Intensive Care Review Board, chairman Professor Jean-Etienne Bazin).

Patient who were hospitalised during March 2020, in a specialised ward or ICU for suspicion of COVID-19 and explored with a chest CT scan as part of their routine care were retrospectively enrolled.

The case definition was based on the presence of a suspected infection of SARS-CoV-2. This definition included fever, new onset of respiratory symptoms (cough, sputum production, dyspnoea, polypnoea, acute respiratory failure, hypoxemia), myalgia or fatigue or any other medical suspicion stated in the patient medical file.

Baseline characteristics of the case patients were extracted from the electronic medical record and included: age, Body Mass Index (BMI), gender, laboratory confirmation of SARS-CoV-2 by RT-PCR, history of arterial hypertension, diabetes, chronic renal failure, clinical status at hospital admission (fever, dyspnoea, SpO<sub>2</sub>, nasal oxygen supplementation, heart rate, mean arterial pressure), routine labs at hospital admission (leucocytes, activated clotting time, prothrombin time).

### CT image acquisition:

All examinations were acquired in 64-row or more CT scanners, with a kV ranging from 80 to 120 kV based on the patient's morphotype (auto-kV). Patients were always positioned supine, with their arms raised above their head whenever possible. Intravenous iodine contrast media was used when pulmonary embolism was suspected to perform CT pulmonary angiography. Lung parenchyma was reconstructed using a hard kernel and millimetric slices.

### Previously described semi-automated lung volume measurement from CT images

As previously described (18), a semi-automated lung volume measurements was performed remotely (e.g. at home) by trained medical imaging technologists using VP-lab© software (Visible Patient©,

Strasbourg, France) (use at distance of the software from Visible Patient Server). The first step consisted of an automatic removal of the extra-thoracic elements followed by an interactive delimitation of the trachea and lungs. Next, a fully automated subsegmentation of 4 zones inside each lung was performed using a colour-encoding system based on CT radio density of voxels (17). Voxels were defined from basic thresholding as non-aerated (-100 to +100 HU), poorly aerated (-500 to -101 HU), normally aerated (-900 to -501 HU) or overinflated (-1 000 to -901 HU). Then, as ground glass opacity (usually having attenuation between -700 and -501 HU) has been extensively reported during COVID-19 infections, the normally aerated regions (-900 to -501 HU) were segmented into ground glass voxels (-700 to -501 HU) vs normally restricted voxels (-900 to -701 HU). The subsegmentation of classically defined normally aerated voxel segment into two subsegments of ground-glass voxels and restricted normally voxels allows for identification of the ground glass specific volume, which are observed frequently in COVID-19 infections (22). The image processing was then continued to remove partial volume effect. A 3D opening (1 voxel in a 6-connected neighbourhood definition) was selected. Supplemental figure 1 illustrates an opening effect on a set of voxels from one of the Fifth zone (here typically a part of the ground-glass voxels on one slide). An opening is defined in Morphological Mathematics as erosion followed by dilation, and the figure shows the efficient removal of partial volume effect or isolated voxels and the preservation of all main 3D components.

The anatomical results of the lung parenchyma segmentation were validated on all cases by an expert senior clinical radiologist. The total volume of each segment of voxels was then calculated. Every CT Scan was double-checked by another engineer, unaware of the clinical part of the charts. The duration of this non-automated process was recorded for each case.

#### Novel Automated lung volume measurement from CT images

Automated lung volume measurements are particularly challenging because of pathological voxels being frequently located at the lung border and having similar grey levels than surrounding tissue. To overcome this problem, we limited our analysis to the voxels corresponding to the normally aerated (-900 to -501 HU) and overinflated (-1 000 to -901 HU) areas. Our fully automatic algorithms (23) was modified by replacing the -300 HU lower threshold used to segment lungs, with a -500 HU threshold.

The resulting fully automatic partial lung segmentation allowed us to next apply an automatic process to compute the ground glass voxels (-700 to -501 HU), the normally restricted voxels (-900 to -701 HU) and overinflated (-1 000 to -901 HU) three subsets of voxels. As previously described, we also applied the same opening to remove the partial volume effect as well as isolated voxels. The duration of this automated process was recorded for each case.

A video clip illustrates the image processing described (supplemental digital content 1).

### Clinical Data

Clinical data were abstracted from the electronic medical record of each patient. Severity of disease was assessed by the maximal respiratory severity assessment based on a seven category ordinal scale (24) during the 7 days following initial CT image acquisition; ICU or death during the 7 days following CT image acquisition: 1-not hospitalised, but unable to resume normal activities; 2-not hospitalised but unable to resume normal activities; 3-hospitalised, not requiring supplemental oxygen; 4-hospitalised, requiring supplemental oxygen; 5-hospitalised, requiring nasal high-flow oxygen therapy, non-invasive mechanical ventilation, or both; 6-hospitalised, requiring ECMO, invasive mechanical ventilation, or both; and 7-death.

To minimise bias during data extraction, all data categories were systematically extracted by the same individual.

### Statistical analysis

Data were described using frequency and proportion (n, %) for categorical variables and mean (sd) for quantitative data. Categorical data were compared using the Fisher exact test. Quantitative data were compared using either Student t-test or Wilcoxon test, depending on the distribution being normal or not. Paired Student t-test was used for within-subject comparison of automated and semi-automated volume measurement duration. The association of the different radiographic measurements and severity score was done using a linear regression model, to estimate the volume variation associated with a one level increase in severity. The effect-size is measured by the coefficient of the linear regression, which gives the change in a given variable for one unit of change in the severity level. The reproducibility of lung volumes (automated or semi-automated) was estimated by computing an intraclass correlation coefficient. No imputations were performed for missing data. Computations were made using 3.5.3 through R-Studio, with the readxl, blandbr and psy packages. A *p*-value less than 0.05 was considered significant.

The sample size was set at 40 consistent with a previously published experimental study focusing on similar endpoints (18).

Based on a reviewer suggestion we made a sensitivity analysis for radiographic measurements and severity score excluding the patients with negative PCRs.



## Results

Fourty patients were screened for study eligibility (Figure 1). Two patients were excluded from the analysis because of technical reasons (see consort Figure 1). One patient was excluded from the clinical outcome correlation because no data regarding clinical outcomes were available at 7 days.

The patients' characteristics are reported in Table 1. There were more patients with a history of chronic renal failure in the ICU group compared to the non-ICU group (24 vs 0% respectively,  $p = 0.03$ ). A positive SARS-CoV-2 RT PCR from a respiratory specimen was observed in 31 of the 37 tested patients (84%).

The results of the CT scan measurements are reported in Table 2. The volume of restricted normally aerated lung volumes was significantly lower in the ICU patients compared to the non-ICU patients in both semi-automated and automated measurements ( $p = 0.048$  and  $0.045$ , respectively). For the classical 4-segment semi-automated lung volume measurements, normally aerated lung volumes were significantly lower in the ICU patients compared to the non-ICU patients (2718 (1027) vs 3377 (1035) ml, respectively,  $p = 0.042$ )

The duration taken to calculate the automated and semi-automated volume measurements were 15 (2) vs 93 (41) min, respectively ( $p = 8.05 \times 10^{-8}$ ). An illustrative representation of the 3-Dimension results of the lung measurements is represented in supplemental Figure 2.

The correlation and Bland-Altman plotting between the semi-automated gold standard and our novel automated experimental lung volume measurements are shown in Figure 2. For both restricted normally aerated and ground-glass opacity, intraclass correlation coefficient between semi-automated and automated methods was superior to 0.99.

The radioclinical association between automated lung volume measurements and the maximal respiratory severity class during the 7 days following the CT scan is represented in Figure 3. The association between the automated measured lung volume and the maximal clinical severity score was statistically significant for the restricted normally aerated ( $p = 0.0097$ , effect size: -385 ml) volumes and for the ratio of ground-glass opacities/restricted normally aerated volumes ( $p = 0.027$ , effect size 3.3).

Radioclinical association between semi-automated lung volumes segmentation and the maximal respiratory severity are represented in supplementary Figure 3. The association between the semi-automated lung volume and the maximal clinical severity score was statistically significant for the normally aerated lung volumes ( $p = 0.015$ ) and for the poorly plus non-aerated lung volumes ( $p = 0.0086$ ).

The proportion patients with a 7-d maximal severity score already reached at day of CT scan is 65 %.

Reviewer based sensitivity analysis are reported in supplementary materials.

## Discussion

Our results suggest that automating a volume measurement of ground-glass opacity and normal lung volumes is feasible and has an excellent correlation with the classical segmentation method. The correlation coefficient, bias and limits of agreement of our automated measurement method compared to the gold standard semi-automated segmentation method were similar to analog validations studies focusing on image-based lung volumes measurement (18, 25). This automated measurement is also correlated with clinical outcome in the next 7 days after CT image acquisition.

Ground-glass opacities are an important radiologic feature of SARS-CoV-2 infections (15, 16, 19, 22, 26, 27). In a systematic review on image findings in COVID-19 gathering 919 cases, ground-glass opacities were the most common features, reported in 88% of the cases (26). CT-scanning is helpful in many cases to diagnose COVID-19 since RT-PCR on respiratory specimens is limited by false negative results, limited availability, and may take hours to days to obtain results (16).

Our goal was to create an automated and quantitative measure of ground-glass opacities from widely available lung CT images, that, as an objective measure of severity of lung injury, could be used clinically and for future research, e.g. eligibility, endpoints, potential confounder.

Initial reports on ground-glass quantification show they are associated with case severity. Li described a visual, semi-quantitative approach to the sum of acute inflammatory lesions involving each lobe summarised in a global semi-quantitative severity score (27). The authors reported an association between the number of lobes involved or the severity score and clinical severity. This non-automated method is challenging to be implemented reproducibly in clinical practice because of the variability and limited reproducibility of the visual semi-quantitative approach. Our novel method produced results consistent with this previous study but is automated and should be easily implemented. We report a positive association between the automated ground glass volume measurement and the clinical severity of our COVID-19 suspected cases (84% PCR+). Therefore, we suggest that our novel automated method can be used clinically and for future research to aid with diagnosis, and as an objective measure of severity of lung injury.

Our study has several limitations. First, as an observational and retrospective study, bias may have contributed to the observed associations. As recommended by the STROBE checklist (20), we made specific efforts to address some anticipated bias, specifically in data extraction procedures. Second, as the time between clinical evolution and the CT scanner acquisition was not standardised, we cannot, based on our results, precisely define the predictive properties associated with the automatic lung volume quantification. A prospective study is underway to explore these potential properties. Third, as this study only involved centres from a single University Hospital, the results

may not be generalisable to other locations. However, we believe that our institutional global management strategy of syndrome surveillance, viral testing, easy access of CT imaging and surge in ICU bed availability reflects many other locations worldwide (13, 16, 28, 29). Fourth, our cohort included some (16%) patients with negative SARS-CoV-2 RT-PCR on respiratory specimens. All patients with available clinical outcome data were included in the analysis in order to test the association between the impaired lung volumes measurement and clinical outcome in a COVID-19 suspect cohort. We believe this pragmatic approach will reflect the real world setting where clinicians will have to make clinical decisions in the context of delayed and possible false PCR negative test results. Fifth, no patients corresponding to primary outcome class 5 were enrolled. As per local policies at the time of the study, the use of non-invasive ventilation or high-flow nasal cannula was restricted. Considering the small sample size, confirmation of these preliminary results are required in larger sample sizes. Last, we did not provide 28 day outcomes because of some loss of follow-up corresponding to medevac required by the local surge of ICU bed (30) during the pandemic.

Our study has several strengths. First, and most importantly, the individual (co-author LS) who performed calculations from the CT images was different from individuals who collected outcome data and performed the statistical analyses. Second, our automated method was using CT scanning technology that is widely available, so this method can be implemented widely. Third, this automated lung volume measurement was associated with a validated respiratory clinical status endpoint (24). This radioclinical assessment for impaired lung volume measurement is a promising concept for various medical fields including infectious diseases, perioperative medicine and critical care. Indeed, we suggest that this automated quantitative analysis could be widely implemented, could be used clinically to aid with diagnosis, and can be used in clinical research as an objective and quantitative measure of severity of lung injury for eligibility assessment, primary or secondary endpoints, or as a potential confounder of disease severity.

## **Conclusion**

In this retrospective cohort study, we assessed the feasibility and preliminary validity of automated, quantitative, impaired lung volumes measurements in a high-density COVID-19 cluster. Ground-glass opacity volume could be potentially used as a potential objective biomarker for COVID-19 lung injury severity.

Funding:

Institutional funding only

Competing interests:

LS is the CEO and stockholder of Visible Patient©

LS, EN, and PD have applied for a patent based on the intellectual content of the automated image-processing algorithm

Acknowledgements:

EN, LS, PD: study design, data extraction, data interpretation, manuscript editing and are guarantor of the paper taking responsibility for the integrity of the work as a whole, from inception to published article; NM: study design, data analysis; manuscript editing; MO JP EBG POL FV FS: data interpretation, manuscript editing

## References

1. Guan W-J, Ni Z-Y, Hu Y, et al.: Clinical Characteristics of Coronavirus Disease 2019 in China. *N Engl J Med* 2020;
2. Chen N, Zhou M, Dong X, et al.: Epidemiological and clinical characteristics of 99 cases of 2019 novel coronavirus pneumonia in Wuhan, China: a descriptive study. *Lancet Lond Engl* 2020; 395:507–513
3. Lu R, Zhao X, Li J, et al.: Genomic characterisation and epidemiology of 2019 novel coronavirus: implications for virus origins and receptor binding. *Lancet Lond Engl* 2020; 395:565–574
4. Coronavirus Disease (COVID-19) Pandemic [Internet]. [cited 2020 Apr 3] Available from: <https://www.who.int/emergencies/diseases/novel-coronavirus-2019>
5. Yang X, Yu Y, Xu J, et al.: Clinical course and outcomes of critically ill patients with SARS-CoV-2 pneumonia in Wuhan, China: a single-centered, retrospective, observational study. *Lancet Respir Med* 2020;
6. Du Y, Tu L, Zhu P, et al.: Clinical Features of 85 Fatal Cases of COVID-19 from Wuhan: A Retrospective Observational Study. *Am J Respir Crit Care Med* 2020;
7. Bhatraju PK, Ghassemieh BJ, Nichols M, et al.: Covid-19 in Critically Ill Patients in the Seattle Region - Case Series. *N Engl J Med* 2020;
8. Huang C, Wang Y, Li X, et al.: Clinical features of patients infected with 2019 novel coronavirus in Wuhan, China. *Lancet Lond Engl* 2020; 395:497–506
9. Barrasa H, Rello J, Tejada S, et al.: SARS-CoV-2 in Spanish Intensive Care Units: Early experience with 15-day survival in Vitoria. *Anaesth Crit Care Pain Med* 2020;
10. McMichael TM, Currie DW, Clark S, et al.: Epidemiology of Covid-19 in a Long-Term Care Facility in King County, Washington. *N Engl J Med* 2020;
11. Verity R, Okell LC, Dorigatti I, et al.: Estimates of the severity of coronavirus disease 2019: a model-based analysis. *Lancet Infect Dis* 2020;
12. Gauss T, Pasquier P, Joannes-Boyau O, et al.: Preliminary pragmatic lessons from the SARS-CoV-2 pandemic from France. *Anaesth Crit Care Pain Med* 2020;
13. Lipsitch M, Swerdlow DL, Finelli L: Defining the Epidemiology of Covid-19 - Studies Needed. *N Engl J Med* 2020;
14. Salehi S, Abedi A, Balakrishnan S, et al.: Coronavirus Disease 2019 (COVID-19): A Systematic Review of Imaging Findings in 919 Patients. *AJR Am J Roentgenol* 2020; 1–7
15. Shi H, Han X, Jiang N, et al.: Radiological findings from 81 patients with COVID-19 pneumonia in Wuhan, China: a descriptive study. *Lancet Infect Dis* 2020; 20:425–434
16. Chua F, Armstrong-James D, Desai SR, et al.: The role of CT in case ascertainment and management of COVID-19 pneumonia in the UK: insights from high-incidence regions. *Lancet Respir Med* 2020;

17. Malbouisson LM, Muller JC, Constantin JM, et al.: Computed tomography assessment of positive end-expiratory pressure-induced alveolar recruitment in patients with acute respiratory distress syndrome. *Am J Respir Crit Care Med* 2001; 163:1444–1450
18. Noll E, Ohana M, Hengen M, et al.: Validation of MRI for Volumetric Quantification of Atelectasis in the Perioperative Period: An Experimental Study in Swine. *Front Physiol* 2019; 10:695
19. Bernheim A, Mei X, Huang M, et al.: Chest CT Findings in Coronavirus Disease-19 (COVID-19): Relationship to Duration of Infection. *Radiology* 2020; 200463
20. von Elm E, Altman DG, Egger M, et al.: The Strengthening the Reporting of Observational Studies in Epidemiology (STROBE) statement: guidelines for reporting observational studies. *Lancet Lond Engl* 2007; 370:1453–1457
21. Toulouse E, Masseguin C, Lafont B, et al.: French legal approach to clinical research. *Anaesth Crit Care Pain Med* 2018; 37:607–614
22. Cheng Z, Lu Y, Cao Q, et al.: Clinical Features and Chest CT Manifestations of Coronavirus Disease 2019 (COVID-19) in a Single-Center Study in Shanghai, China. *AJR Am J Roentgenol* 2020; 1–6
23. Soler L, Nicolau S, Hostettler A, et al.: Computer assisted Digestive Surgery. In: Computational Surgery and Dual Training. 2010. p. 139–153.
24. Cao B, Wang Y, Wen D, et al.: A Trial of Lopinavir-Ritonavir in Adults Hospitalized with Severe Covid-19. *N Engl J Med* 2020;
25. Ball L, Braune A, Corradi F, et al.: Ultra-low-dose sequential computed tomography for quantitative lung aeration assessment-a translational study. *Intensive Care Med Exp* 2017; 5:19
26. Salehi S, Abedi A, Balakrishnan S, et al.: Coronavirus Disease 2019 (COVID-19): A Systematic Review of Imaging Findings in 919 Patients. *Am J Roentgenol* 2020; 1–7
27. Li K, Fang Y, Li W, et al.: CT image visual quantitative evaluation and clinical classification of coronavirus disease (COVID-19). *Eur Radiol* 2020;
28. Bouadma L, Lescure F-X, Lucet J-C, et al.: Severe SARS-CoV-2 infections: practical considerations and management strategy for intensivists. *Intensive Care Med* 2020; 46:579–582
29. Yang X, Yu Y, Xu J, et al.: Clinical course and outcomes of critically ill patients with SARS-CoV-2 pneumonia in Wuhan, China: a single-centered, retrospective, observational study. *Lancet Respir Med* 2020;
30. Noll E, Muccioli C, Ludes P-O, et al.: Surgical Support for Severe COVID-19 Patients: A Retrospective Cohort Study in a French High-Density COVID-19 Cluster. *Surg Innov* 2020; 1553350620954571

## Figures legends

### Figure 1: Study Flowchart

CT: Computed Tomography

### Figure 2: Correlation and Bland-Altman Plotting of Measured lung volumes based on semi-automated and automated procedures

Correlation plotting of lung volumes measured with Semi-automated or Automated procedures for restricted Normally aerated densities (A) and Ground-Glass densities (C). Bland-Altman plotting of lung volumes measured with Semi-automated or Automated procedures for restricted Normally aerated densities (B) and Ground-Glass densities (D): dotted horizontal bar with blue, green and red font are for mean difference, upper and lower limit of agreements, respectively. Coloured fonts are for 95 % Confidence Interval

### Figure 3 Radioclinical associations of automated lung volumes measurements

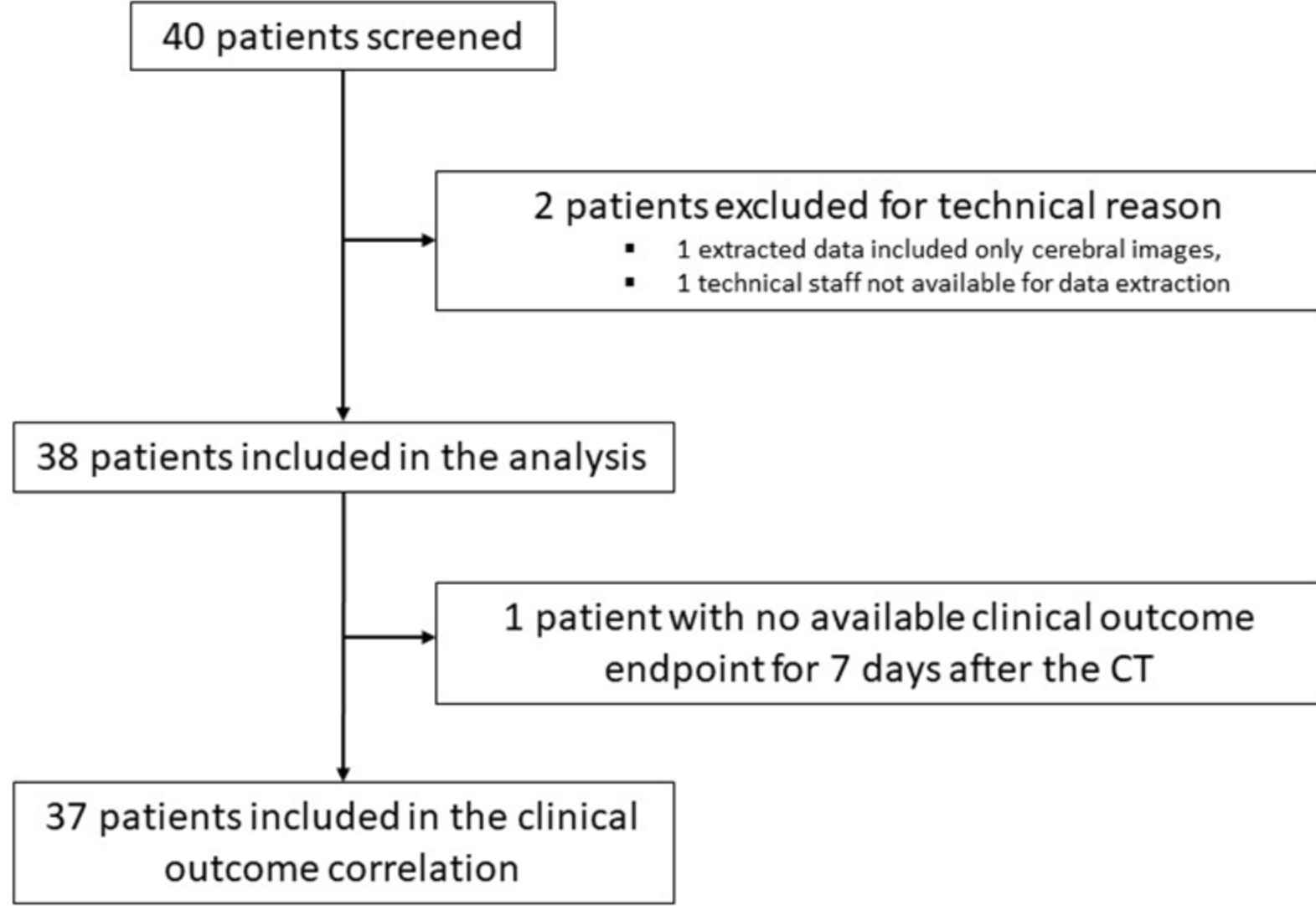
Measured lung volumes for the automated process of (A): Ground-glass opacities; (B) Restricted Normally Aerated and for (C) the ratio of Ground-glass opacities and Restricted Normally Aerated volumes for those with class 3,4 and 6 maximal respiratory severity during the 7 days following the CT scan. The association between the automated measured lung volumes and the maximal clinical severity score was statistically significantly different for the restricted normally aerated ( $p = 0.0097$ ) volumes and for the ratio of ground-glass opacities/restricted normally aerated volumes ( $p = 0.027$ ). No patients in our cohort were classified as 1, 2, 5 or 7 on this scale.

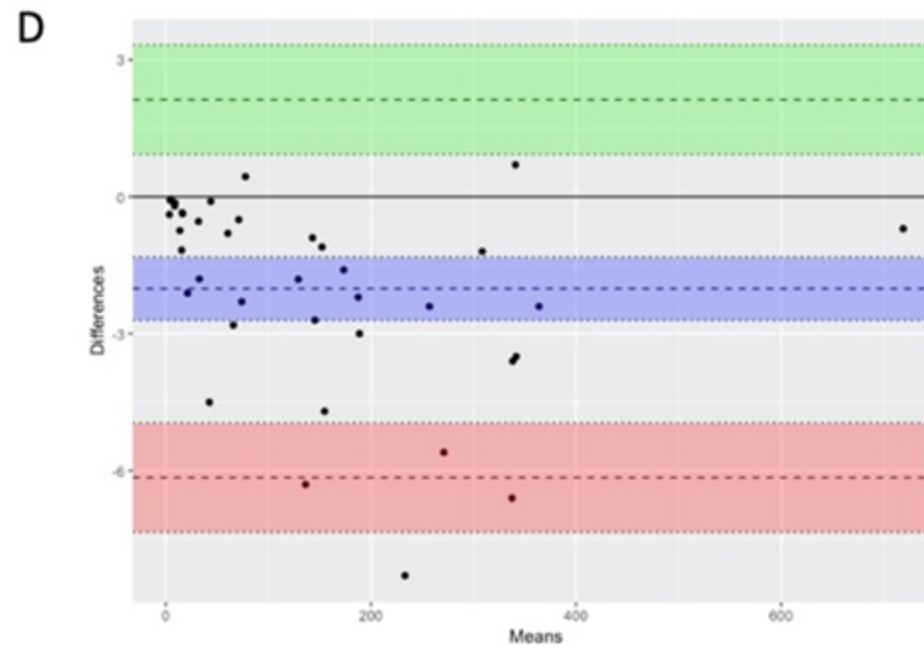
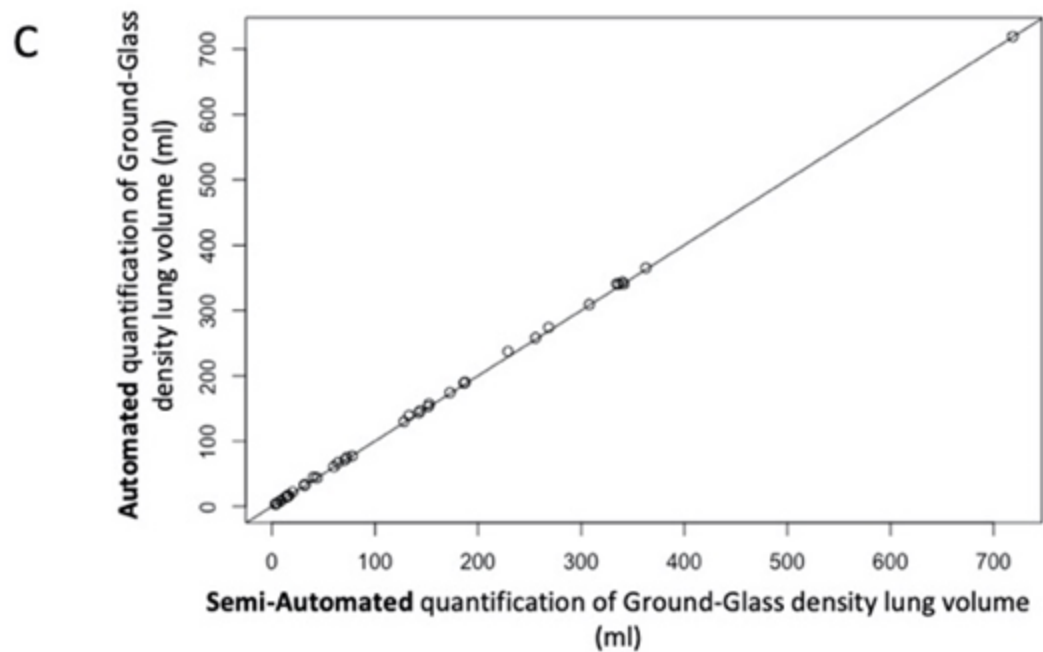
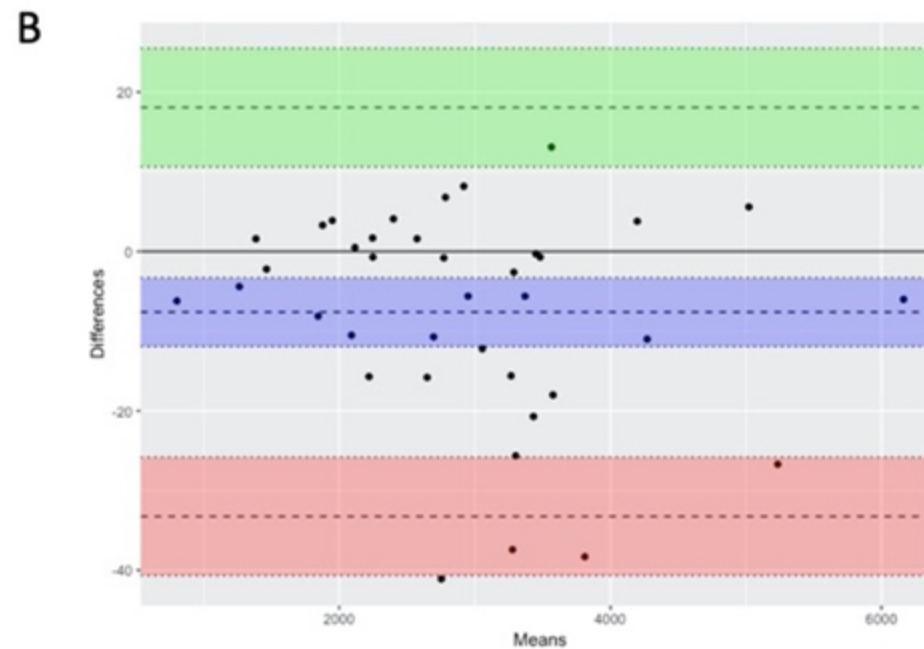
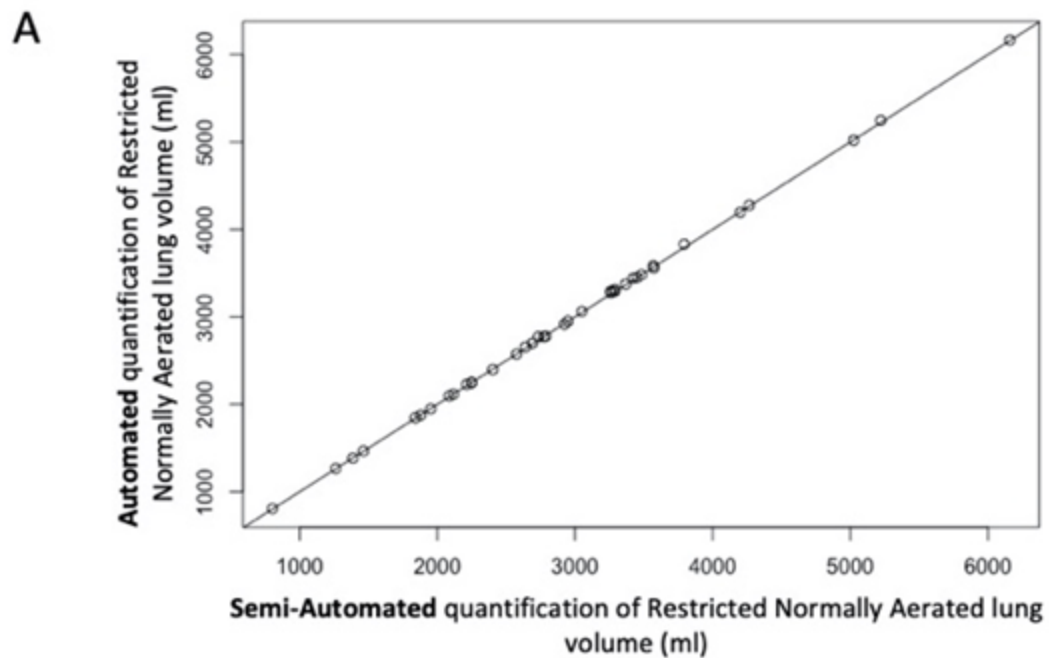


**Table 2: Computed Tomography Measurements**

Variables	ALL (n=38)	NON-ICU (n=21)	ICU (n=17)	NON-ICU vs ICU p
Duration between hospital admission and CT scan (days)	-0.18(3.0)	0.14 (0.36)	-0.59(4.51)	0.40
Duration between CT scan and ICU admission	NA	NA	1.41(4.77)	NA
Semi-automated quantification of pulmonary ground glass volume (ml)	145 (151)	125 (131)	168 (174)	0.39
Automated quantification of pulmonary ground glass volume (ml)	147 (152)	127 (133)	171 (174)	0.45
Semi-automated quantification of pulmonary restricted normally aerated lung volume (ml)	2938 (1104)	3252 (1006)	2549 (1124)	<b>0.048</b>
Automated quantification of pulmonary restricted normally aerated lung volume (ml)	2945 (1106)	3261 (1007)	2555 (1127)	<b>0.045</b>
Automated quantification of ground glass opacity/restricted normally aerated (%)	7.1 (10.7)	4.0 (4.3)	10.8 (14.7)	0.19
<b>SEMI-AUTOMATED 4 SEGMENTS LUNG VOLUME QUANTIFICATION</b>				
Overinflated lung volume (ml)	477 (574)	549 (635)	389 (493)	0.11
Normally aerated lung volume (ml)	3082 (1071)	3377 (1035)	2718 (1027)	<b>0.042</b>
Poorly aerated lung volume (ml)	266 (236)	208 (163)	337 (293)	0.23
Non-aerated lung (ml)	138 (214)	72 (76)	219 (294)	0.20

Computed Tomography (CT) measurements; ICU: Intensive Care Unit; ml: milliliters





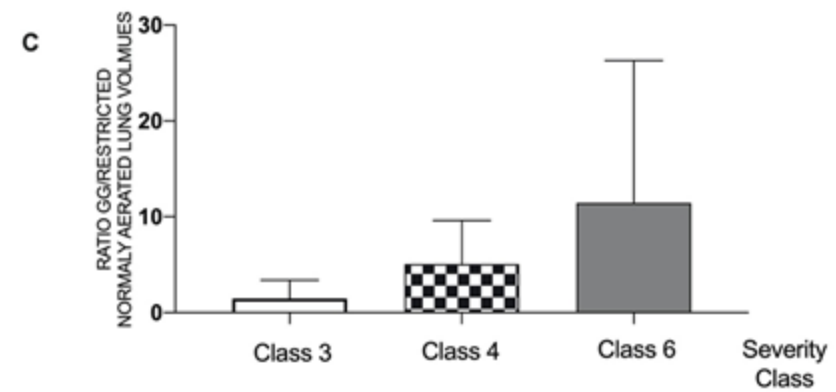
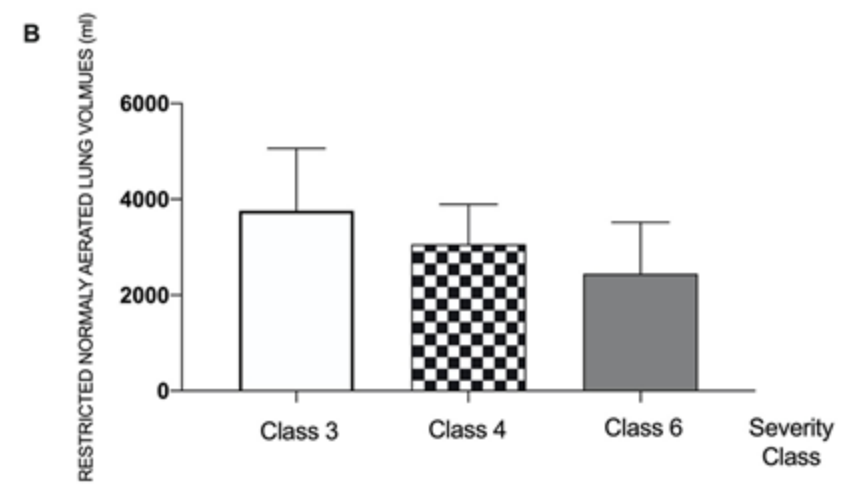
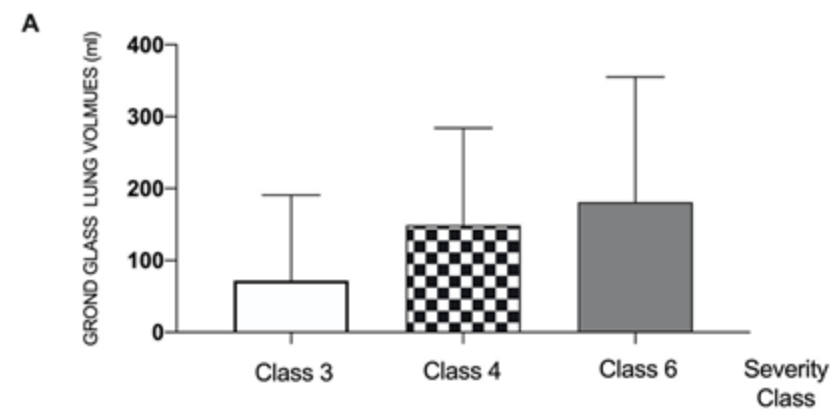


**Table 1 : Patient demographics**

Variables	ALL (n=38)	Non-ICU (n=21)	ICU (n=17)	Non-ICU vs ICU p
Age, year (SD)	64 (11)	62 (14)	67 (6)	0.16
BMI, kg/m2 (SD)	29 (6)	29 (6)	30 (5)	0.65
Gender (F/M %)	27	33	18	0.46
<b>Medical History</b>				
Arterial Hypertension, n (%)	21 (55)	10 (48)	11 (65)	0.34
Diabetes, n (%)	14 (37)	9 (43)	5 (29)	0.51
Chronic Renal Failure, n (%)	4 (11)	0 (0)	4 (24)	<b>0.03</b>
<b>Clinical status at Hospital admission</b>				
Body Temperature	37.5 (1.0)	37.5 (1.1)	37.5 (1.0)	0.99
Dyspnea	26/35 (74)	15/21 (71)	11/14 (79)	0.71
SpO2	95 (3)	95 (3)	95 (3)	0.62
Heart Rate (bpm)	87 (15)	90 (15)	84 (16)	0.32
Mean Arterial Pressure (mmHg)	94 (13)	95 (12)	92 (14)	0.51
<b>Routine labs at Hospital Admission</b>				
SARS-CoV-2 RT-PCR (%)	31(84)	16 (80)	15(88)	0.66
Leucocytes (G/L)	7.6 (3.1)	7.1 (3.0)	8.3 (3.1)	0.21
PT (%)	86 (13)	84 (15)	88 (12)	0.50

Patient demographics, medical history, clinical status and routine labs at admission in the patient not admitted to the ICU (Non-ICU) or admitted to the ICU (ICU) during their hospitalization. BMI: Body Mass Index, SD: Standard Deviation; F/M: Female/Male; SpO2: peripheral capillary chain reaction, bpm: beat per minute; mmHg : millimeter of mercury; G/L: giga per liter; PT: prothrombin time.